Acta Crystallographica Section D
Biological Crystallography
ISSN 0907-4449

The 1.45 Å resolution structure of the cryptogein–cholesterol complex: a close-up view of a sterol carrier protein (SCP) active site

Marie-Bernard Lascombe,[a]* Michel Ponchet,[b] Paul Venard,[b] Marie-Louise Milat,[c] Jean-Pierre Blein[c] and Thierry Prangé[a]

[a]Laboratoire de Cristallographie et RMN Biologiques (UMR-8015, CNRS), Faculté de Pharmacie, 4 Avenue de l'Observatoire, 75270 Paris CEDEX 06, France, [b]IPMSV Phytopathologie, INRA, BP 2078, 06606 Antibes CEDEX, France, and [c]UMR-692 INRA, Université de Bourgogne, Phytopharmacie et Biochimie des Interactions Cellulaires, BP 86510, 21065 Dijon CEDEX, France

Correspondence e-mail: lascombe@pharmacie.univ-paris5.fr

Received 17 February 2002
Accepted 3 July 2002

PDB Reference: cryptogein–cholesterol complex, 1lri, r1lrisf.

Cryptogein is a small 10 kDa elicitor produced by the phytoparasitic oomycete *Phytophthora cryptogea*. The protein also displays a sterol carrier activity. The native protein crystallizes in space group $P4_122$, with unit-cell parameters $a = b = 46.51$, $c = 134.9$ Å (diffraction limit: 2.1 Å). Its complex with cholesterol crystallizes in space group $C222_1$, with unit-cell parameters $a = 30.96$, $b = 94.8$, $c = 65.3$ Å and a resolution enhanced to 1.45 Å. The large inner non-specific hydrophobic cavity is able to accommodate a large variety of 3-β-hydroxy sterols. Cryptogein probably acts as a sterol shuttle helping the pathogen to grow and complete its life cycle.

1. Introduction

Elicitins are proteins secreted by the phytopathogenic *Phytophthora* spp. These proteins are elicitors of plant resistance (Bonnet *et al.*, 1996; Keller *et al.*, 1999); they bind to receptors located on the plant plasma membrane and trigger a complex signal-transduction pathway (Ponchet *et al.*, 1999). Their sequences are very similar (Fig. 1) and, according to their pI, they are divided into two classes, acidic (α) or basic (β) elicitins. Elicitins have also been characterized as extracellular sterol carrier proteins (Mikes *et al.*, 1997, 1998) and are able to catalyze sterol transport between micelles and artificial and/or natural membranes (Vauthrin *et al.*, 1999). As such, they are non-specific and accommodate a large panel of phytosterols as well as fatty acids, which compete for binding as recently demonstrated (Osman, Mikes *et al.*, 2001). Elicitin structures have been investigated by both crystallography (Boissy *et al.*, 1996) and NMR (Fefeu *et al.*, 1997, 1998; Gooley *et al.*, 1998). The X-ray three-dimensional structures of two basic elicitins, cryptogein (Boissy *et al.*, 1996) and cinnamomin (Archer, Rodrigues, Aurelio, Biemans *et al.*, 2000; Archer, Rodrigues, Aurelio, Cravador *et al.*, 2000), have been reported. In addition, an unexpected ergosterol complex was also reported in the case of a cryptogein mutant (Boissy *et al.*, 1999). In the presence of cholesterol, native cryptogein displays a drastic modification of its crystal habit with increased stabilization and enhanced resolution. The aim of this study is to determine accurately the parameters involved in sterol capture by elicitins.

2. Experimental

2.1. Crystallization, data collection and data processing

Cholesterol was purchased from Sigma–Aldrich Co.; cryptogein was isolated and purified by chromatographic

```
          10        20        30        40        50
Cac  ATCTSSQQTA AYVALVSILS DTSFNQCSTD SGYSMLTATS LPTTAQYTLM
Cap  ATCTTTQQTA AYVALVSILS DSSFNQCATD SGYSMLTATA LPTTAQYKLM
Par  TTCTTTQQTA AYVALVSILS DTSFNQCSTD SGYSMLTATS LPTTEQYKLM
Mgmα TTCTSTQQTA AYVTLVSILS DSSFNQCATD SGYSMLTATA LPTTAQYKLM
Dreα TTCTSTQQTA AYVTLVSILS DSSFNQCATD SGYSMLTATA LPTDAQYKLM
Inf  TTCTTSQQTV AYVALVSILS DTSFNQCSTD SGYSMLTATS LPTTEQYKLM
Dreβ TACTSTQQTA AYTTLVSILS DSSFNKCASD SGYSMLTAKA LPTTAQYKLM
Mgmβ TACTTTQQTA AYKTLVSILS ESSFNQCSKD SGYSMLTATA LPTNAQYKLM
Cin  TACTATQQTA AYKTLVSILS ESSFSQCSKD SGYSMLTATA LPTNAQYKLM
Cry  TACTATQQTA AYKTLVSILS DASFNQCSTD SGYSMLTAKA LPTTAQYKLM
     *+CT:*QQT* AY++LVSILS *+SF**C+*D SGYSMLTA** LPT**QY*LM

          60        70        80        90       100
Cac  CGSTACKTMI NKIVSLNPPN CELTVPTSGL VLNVYSYANG FSTTCSSL
Cap  CASTACNTMI TKIVSLNPPD CELTVPTSGL VLNVYSYANG FSATCASL
Par  CASTACKTMI NKIVTLNPPD CELTVPTSGL VLNVFTYANG FSSTCASL
Mgmα CASTACNTMI NKIVTLNPPD CELTVPTSGL VLNVYSYANG FSATCASL
Dreα CSSTACNTMI KKIVSLNAPN CDLTVPTSGL VLNVYEYANG FSTKCASL
Inf  CASTACKTMI NKIVSLNAPD CELTVPTSGL VLNVYSYANG FSSKCASL
Dreβ CASTACNTMI KKIVSLNPPN CDLTVPTSGL VLNVYEYANG FSTKCASL
Mgmβ CASTACKSMI NKIVVLNPPD CDLTVPTSGL VLDVYTYANG FSTKCASL
Cin  CASTACNTMI KKIVALNPPD CDLTVPTSGL VLDVYTYANG FSSTCASL
Cry  CASTACNTMI KKIVTLNPPN CDLTVPTSGL VLNVYSYANG FSNKCSSL
     C*STAC+*MI +KIV+LN*P+ C+LTVPTSGL VL*V*+YANG FS::C*SL
```

Figure 1
Amino-acid sequence alignment for some elicitins (α = acidic, above the line; β = basic, below). Symbols: Cac, cactorin from *P. cactorum* (Huet *et al.*, 1993); Cap, capsicein from *P. capsici* (Ricci *et al.*, 1989); Par, parasiticein from *P. parasitica* (Mouton-Peronnet *et al.*, 1995); Mgmα and Mgmβ, megaspermins from *P. megasperma megasperma* (Huet & Pernollet, 1993); Dreα and Dreβ, dreschlerin from *P. dreschleri* (Huet *et al.*, 1992); Inf, infestin from *P. infestans* (Kamoun *et al.*, 1993); Cry, cryptogein (Ricci *et al.*, 1989); Cin, cinnamomin from *P. cinnamomi* (Huet & Pernollet, 1989). Consensus (last line) is labelled as usual: a dot (.) if occurrence is $\geq$20%, a colon (:) if $\geq$0%, a plus sign (+) if $\geq$60%, a star (*) if $\geq$80% and the residue symbol if conserved. The residues lining the cavity in cryptogein (cry) are shaded in grey. These residues are conserved among all elicitins.

methods from the culture filtrate of *P. cryptogea* as previously described (Bonnet *et al.*, 1996). Lyophilized cryptogein (2.5 mg) was incubated in sodium acetate buffer (50 µl, 50 m*M*, pH 4.7) with a large excess of cholesterol (1 mg) under overnight agitation. Excess cholesterol was removed by centrifugation and the solution set to crystallize following the hanging-drop method. The crystallizing agent was 4.5 *M* sodium chloride. Large prismatic crystals developed in about 3 d.

Diffraction data were collected at 278 K on the W32 wiggler beamline (Fourme *et al.*, 1992) at the LURE synchrotron facility, Orsay (France) using a MAR Research 345 mm image-plate detector and the integrating program *MOSFLM* (Leslie, 2001) interfaced with the *CCP*4 suite of program (Collaborative Computational Project, Number 4, 1994). The native space group is $P4_122$, but the cholesterol derivative crystallizes in space group $C222_1$, with unit-cell parameters a = 30.97, b = 95.02, c = 65.42 Å, one molecule in the asymmetric unit and a solvent content of 39%. 64 233 intensities were processed and reduced to 17 432 independent structure factors ($R_{\rm merge}$ = 3.9%) within the 10.0–1.45 Å resolution range [$R_{\rm merge}$ = 21.3% in the last resolution shell, with $I/\sigma(I)$ = 4.6]. Completeness is 96%.

Table 1
Final refinement statistics.

Atoms	
Protein	716
Solvent	99 waters, one Cl^-
Cholesterol	28
Refinement (No. of reflections in parentheses)	
Resolution range (Å)	10.0–1.45
No. of parameters/restraints	7573/9193
R factor for observed data (%)	12.7 (16165 $F \geq 4\sigma$)
R factor for all data (%)	13.0 (17432)
Free R factor for 8% of observed data (%)	16.8 (992)
R.m.s. deviations (No. of deviations in parentheses)	
Bond length (Å)	0.012 (805)
Bond angles (Å)	0.03 (1108)
Planes	0.03 (247)
Non-zero chiral volumes (Å^3)	0.06 (135)
Zero chiral volumes (Å^3)	0.06 (123)
Average isotropic $\langle B \rangle$ values† (Å^2) (No. of atoms in parentheses)	
Main chain	18.7 (393)
Side chain	24.5 (323)
Cholesterol	19.0 (28)
Water molecules	35.8 (99)
Min./max. residuals in final Fourier map (e$^-$)	−0.28/+0.31

† Recalculated from anisotropic U_{ij} components.

2.2. Refinement

The starting model was the structure of a cryptogein mutant at 2.15 Å resolution without the ergosterol ligand (PDB code 1bxm; Boissy *et al.*, 1999). As the cholesterol complex parameters are not strictly isomorphous to the 1bxm structure, a first round of molecular replacement and a rigid-body refinement was performed with the *AMoRe* program (Navaza, 1994). The refinements were conducted using the *SHELXL* program (Sheldrick & Schneider, 1997) with restrained bond distances, angle distances and isotropic thermal factors. Water molecules were located on Fourier-difference maps and continuously updated during the refinement procedure (B factors were not allowed to be greater than 60 Å^2). This was performed using the *ARP*/*wARP* recycling procedure (Lamzin & Wilson, 1997). Planar rings and chiral volumes were also constrained. A few amino-acid residues showed clear alternate positions; they were refined with the sum of their occupancy factors constrained to unity. Refinement of the structure was continued using restrained anisotropic thermal factors for individual atoms. The procedure ended with R_w = 12.7% (for 16 165 structure factors above 4σ), R_w = 13.0% (all data), R_{w2} = 31.2% (calculated on F^2), $R_{\rm free}$ = 16.8% (using 8% of the data). The statistics of the refinement are reported in Table 1. The Ramachandran plot (Ramachandran *et al.*, 1963) was calculated with *PROCHECK* (Laskowski *et al.*, 1993). All residues but three are in the most favoured regions.

3. Results and discussion

The refined model of the structure consists of 98 residues, one chlorine ion, 99 water molecules and one cholesterol molecule

Figure 2
The cholesterol molecule in the cavity of cryptogein. The unique polar contact of cholesterol is between the phenolic group of Tyr47 buried at the bottom of the inner cavity and the 3β-hydroxyl function of the sterol (*MOLSCRIPT*/*RASMOL* programs; Kraulis, 1991; Merritt & Bacon, 1997).

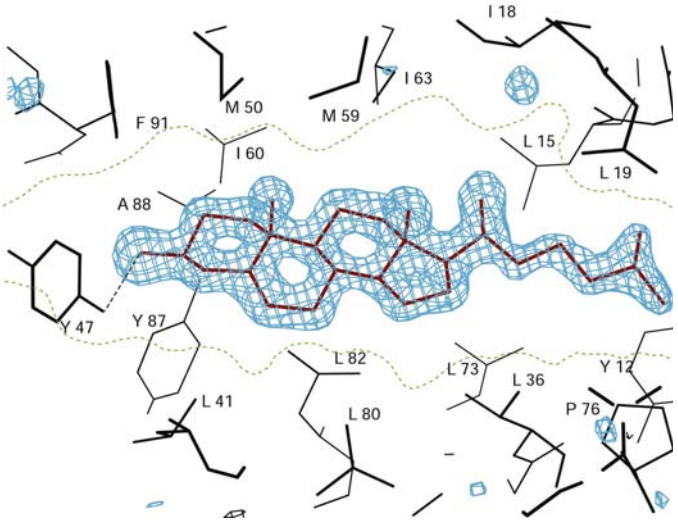

Figure 3
Electron density (omit map) of cholesterol in the cavity contoured at 2.5σ, calculated with refined phases at 1.45 Å resolution.

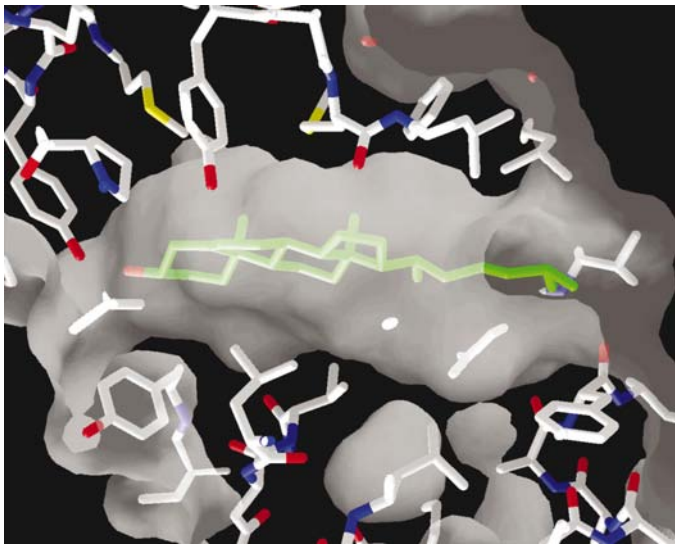

Figure 4
The hydrophobic cavity formed by side chains of amino acids in the centre of cryptogein (*GRASP* program; Nicholls *et al.*, 1991).

(Fig. 2). Fig. 3 shows an omit map calculated after removing the cholesterol contribution. At 1.5 Å resolution, residues Thr65, Ser92 and Asn93 clearly show alternate orientations.

The MALDI–TOF mass spectrum analysis of cryptogein indicates that the wild-type protein is heterogeneous, showing two distinct monoisotopic masses with a difference in mass of 12 Da. This heterogeneity does not exist in the protein expressed in *Pichia pastoris* (Osman, Vauthrin *et al.*, 2001), but crystallization of the heterologous cryptogein is more difficult as it contains an additional N-terminal short segment which drastically modifies the crystal formation and stability. The same problem was encountered in the previous reported K13H mutant (Boissy *et al.*, 1999). At a resolution of 1.45 Å, it may be possible to determine where any misattribution or heterogeneity might be present along the chain. Hence, in helix 1 at the Thr6 position, the electron density is likely to be in favour of a serine as observed in infestin or cactorin (Fig. 1). This observation was also pointed out in the native structure (Boissy *et al.*, 1996). Another misattribution may also occur for Asn93, which was actually modelled as a disordered residue. The bifurcated density observed here could be either a valine or a threonine, as in cactorin or dreschlerin. A more detailed analysis of the heterogeneity of the purified extracted cryptogein is under way and will be reported elsewhere.

The cryptogein structure comprises five α-helices, two short β-strands and two loops associated in a bowl-shaped structure by three disulfide bonds. The topology of these elements builds a large hydrophobic cavity which constitutes the main characteristic of cryptogein (Figs. 3 and 4).

3.1. The central hydrophobic cavity

This cavity has the shape of an elongated tube about 19 Å in length and 9 Å in diameter (Fig. 4). One end of the cavity points to the surface of the protein. It is closed by two loops: the first (termed the ω-loop) includes residues 32–43 and the second residues 75–80. This forms a jaw-like motif with apparent flexibility. The other extremity of the cavity ends at the polar Tyr47 (Figs. 2 and 4). The phenolic OH group of Tyr47 is involved in a strong hydrogen bond with the 3β-hydroxyl group of the steroid (d = 2.59 Å). This bond is also observed in the 2.15 Å resolution structure of the ergosterol complex of the T1G/A2T/K13H cryptogein mutant (Boissy *et al.*, 1999) and appears to be essential for binding. When Tyr47 is mutated, the protein loses most of its ability to capture sterols. This is illustrated by the two mutants Y47F and Y47G described by Osman, Vauthrin *et al.* (2001). In addition, we have found that when the 3β-hydroxyl function of the sterol is modified or substituted as in cholesteryl acetate, bromide or iodide, no complex can be formed.

Table 2
Hydrophobic contacts between side chains of the cryptogein amino acids lining the cavity and the cholesterol molecule (range: 3.6–4.3 Å), in addition to the single polar hydrogen bond between Tyr47 OH and the O(3) hydroxyl function of cholesterol (d = 2.59 Å).

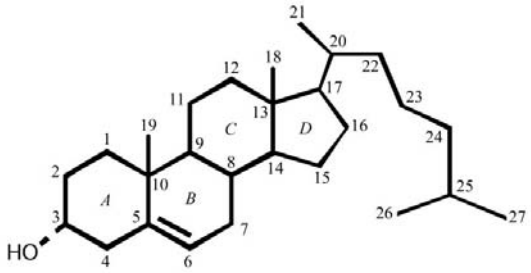

Residue atom	Cholesterol atom	Distance (Å)
Ring *A*		
Phe91 CD1	C(2)	4.08
Tyr87 CD1	C(3)	4.21
Tyr87 CB	C(1)	4.14
	C(2)	4.04
	C(3)	4.00
Tyr87 O	C(2)	3.78
Ile60 CD1	C(1)	3.97
	C(2)	3.87
	C(19)	4.01
Met50 CE	C(19)	4.15
Met59 CE	C(19)	3.88
Tyr47 OH	C(3)	3.50
	C(4)	3.62
Pro42 CD	C(4)	3.78
Ring *B*		
Pro42 CD	C(6)	4.13
Leu41 CD2	C(6)	4.19
Tyr33 OH	C(6)	3.59
	C(7)	3.69
Leu82 CD1	C(6)	4.02
	C(7)	4.02
Leu80 CD2	C(7)	3.98
Tyr33 CE2	C(6)	3.98
	C(7)	4.14
Pro42 CD	C(6)	3.78
Ring *C*		
Ile63 CD1	C(11)	3.79
	C(12)	3.96
Ring *D*		
Met35 C	C(15)	4.10
Met35 SD	C(18)	3.91
Met35 CB	C(15)	4.15
	C(18)	4.13
Phe24 CE1	C(18)	4.07
Val75 CG2	C(16)	4.04
Side chain		
Leu15 CD2	C(21)	4.15
Leu36 CD2	C(23)	4.09
	C(24)	4.00
Tyr12 O	C(26)	3.79
Leu15 CB	C(26)	4.28
Val16 CA	C(26)	3.94

The cavity is highly hydrophobic, mostly lined by leucines (Leu15, Leu19, Leu36, Leu41, Leu82) isoleucines (Ile60 and Ile63) and other similar residues (Val84, Ala38, Phe24, Phe91, Ala88). The two methyl groups [C(18) and C(19)] of the sterol are oriented toward secondary cavities delineated by the side chains of Met35 and Ile18 for C(18), and Met50 and Met59 for C(19). The C(25)–C(27) isopropyl group of cholesterol protrudes from the surface of the cavity (Fig. 4) with only loose interactions. Table 2 summarizes the closest contacts between the cholesterol molecule and the hydrophobic residues of the cavity.

A method to determine and probe the hydrophobic character of cavities is the use of xenon, a technique that has recently been reported (Prangé *et al.*, 1998; Quillin *et al.*, 2000). In the case of cryptogein, no xenon signature is present in the X-ray structure at xenon pressures of up to 2 MPa. This is not surprising since the cavity is too wide to meet the usual requirements in size and shape for xenon binding. It is probable that the use of NMR spectroscopy with polarized xenon would reveal interactions with inner residues of the cavity, following the technique described by Landon *et al.* (2001) for the case of a lipid-transport protein (LTP).

Although located in a completely different environment, the cavity has some analogies with other SCP protein binding sites. Cryptogein and Scp-2 (Choinowski *et al.*, 2000; Haapalainen *et al.*, 2001) proteins are structurally unrelated and show no sequence homology. However, these two classes of proteins are very similar with respect to the size, shape and hydrophobicity of their cavities. Further close transport proteins with equivalent function and mechanism are OBPs (odorant-binding proteins; Bianchet *et al.*, 1996; Vincent *et al.*, 2000). In such proteins, the cavity is large enough to accommodate small organic ligands such as mono- or sesquiterpenes or other equivalent synthetic organic molecules in a non-specific manner. Again, comparisons cannot be drawn further as OBP cavities are open β-barrel substructures embedded in a larger protein structure and lacking a closing lid or any other equivalent motif. OBPs also have a wider range of putative ligands at the micromolar scale. In the case of cryptogein, only a selective range of molecules, 3β-hydroxy steroids, are accepted owing to the specific interaction with the Tyr47 hydroxyl group and also owing to the selective anchoring of a C17 side chain.

3.2. Free state *versus* bound state comparisons

The mechanism by which the sterol enters the cavity is of interest. On one hand, the protein acts as a shuttle to supply lipids and especially sterols that the pathogen cannot synthesize; on the other hand, the loading of cryptogein is a prerequisite to trigger its necrotic (elicitor) activity *in planta* (Osman, Vauthrin *et al.*, 2001). In this context, the transport must be as non-specific as possible for the cavity to accommodate most of the natural phytosterols. In addition, the sterol must be trapped but also released efficiently. A recent molecular-dynamics study (Demaret *et al.*, 2000) pointed out the role of the ω-loop in the recognition step, with a special mention of residue Lys13 as the way the sterol enters the cavity, although the K13H mutation does not significantly alter either the binding or the biological activity, as demonstrated previously (Boissy *et al.*, 1999).

The least-squares superimposition of the free-state and bound-state C^{α} tracings of cryptogein was calculated. The r.m.s. differences are reported in Fig. 5(*a*) as a function of the sequence. The figure shows that larger systematic displacements (∼1.5–3 Å) occur at the beginning of the sequence in helices 1*a* and 1*b* (residues 5–32); particular mention should be made of residues 14–15, which swing out upon binding of cholesterol (r.m.s. = 3 Å) and act as a hinge point between the two first helices. A second region with a large difference (2.7 Å r.m.s. for Ser34) occurs in the ω-loop, which is displaced by the loading. Surprisingly, C^{α} atoms of the rest of the structure and especially of the second loop closing the cavity are within 0.5–1.5 Å r.m.s deviation, an indication that the cavity itself is not greatly affected by the presence of cholesterol.

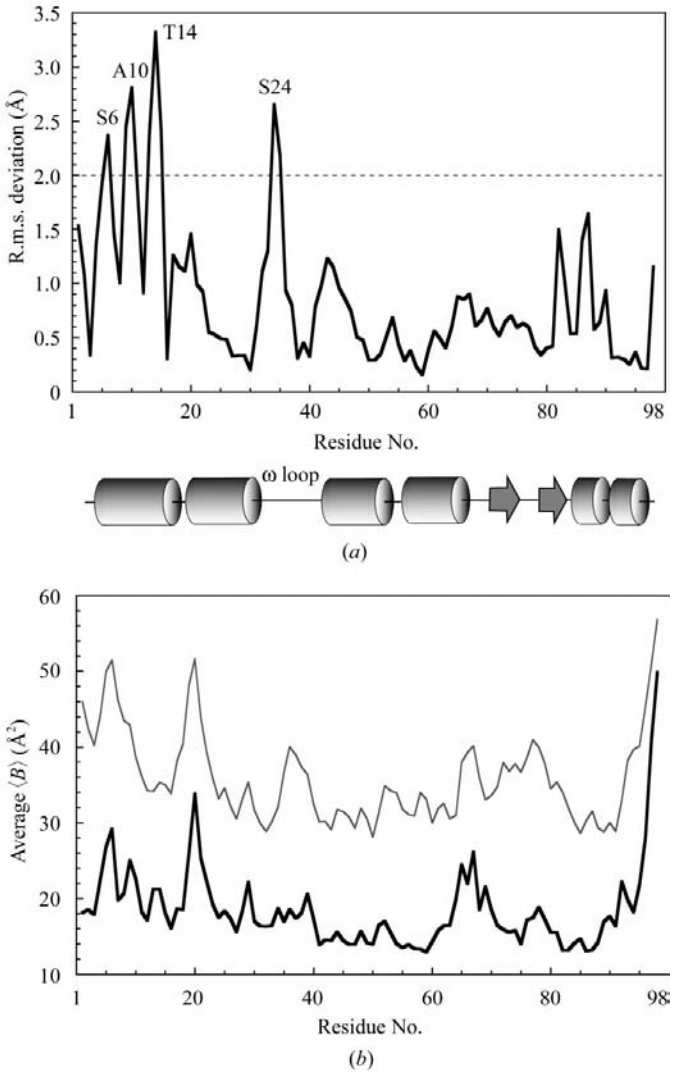

Figure 5
Comparisons between uncomplexed and complexed cryptogein structures. (*a*) R.m.s. deviations of C^{α} atoms *versus* the sequence (program *LSQKAB*; Collaborative Computational Project, Number 4, 1994). The most affected residues are labelled. (*b*) The average $\langle B \rangle$ factors in residues (program *BAVERAGE*; Collaborative Computational Project, Number 4, 1994). The light-grey curve represents the free state; the bold tracing the cholesterol-loaded protein. The average shift between the two curves (∼15 Å^2) represents the stabilization effect of cholesterol binding. Both crystals (free and complexed) were recorded under the same conditions: T = 278 K, wet capillaries.

Indeed, a number of amino-acid side chains that point towards the cavity are affected by the presence of cholesterol. This is the case for Tyr87 (r.m.s. deviations of ∼7–8 Å for side-chain atoms) which rotates about its χ_1 bond angle and moves to a less hindered place. This is also the case for side chains of previously mentioned Leu15 and Met35 (r.m.s. deviations of ∼4 Å).

The size of the cryptogein cavity was estimated as 570 (30) Å^3 in the native protein. For the complex, when the cholesterol ligand is removed the calculated size is about the same value [560 (30) Å^3]; the difference is within standard deviation and too small to correspond to the van der Waals molecular volume of cholesterol (∼280–350 Å^3). This shows that the cavity is initially present in cryptogein and is not modified following the binding of cholesterol.

Comparisons of the average B values between the free and complexed cryptogein are given in Fig. 5(*b*). Unexpectedly, the mobility in the two loops closing the cavity remain reasonably low and close to the overall $\langle B \rangle$ factor of the protein. The corresponding electron densities of these two loops are very clear and interpretable, with the exception of one side chain (Lys39). Indeed, the two B-factor curves are not identical because of the enhanced resolution between the free and the bound state. However, they remain very similar.

4. Conclusions

Cryptogein, despite its small size, displays a large inner hydrophobic cavity, which is polar at its base, assuming a crucial role for the buried Tyr47 residue (its mutation abolishes the SCP character of cryptogein). This cavity is closed by a jaw-like motif (loops 32–43 and 75–80), which apparently plays a role in the mechanism of capture/release. This study shows that the N-terminal helix is also involved in the stabilization and formation of the complex once the sterol enters the protein. The cavity is rather loose in conformation; its size does not vary greatly upon loading and as such may accommodate a variety of sterols as well as fatty acids (Osman, Mikes *et al.*, 2001). Cryptogein probably acts as a shuttle for the oomycete to find elements it cannot synthesize and thus constitutes an essential vector in the parasitism of *Phytophthora* spp. Further, the biological toxicity (leaf necrosis) of cryptogein is considerably enhanced when the protein is preloaded with a sterol. The present study illustrates the drastic stabilization of the protein crystal structure upon binding of cholesterol. This feature is also observed in the case of oligandrin, an elicitin-like protein isolated from *Phythium oligandrum* (Lascombe *et al.*, 2000) belonging to another class of oomycetes.

References

Archer, M., Rodrigues, M. L., Aurélio, M., Biemans, R., Cravador, A. & Carrondo, M. A. (2000). *Acta Cryst.* D**56**, 363–365.

Archer, M., Rodrigues, M. L., Aurélio, M., Cravador, A. & Carrondo, M. A. (2000). *Acta Cryst.* A**56** (Supplement), s269.
Bianchet, M. A., Bains, G., Pelosi, P., Pevsner, J., Snyder, S. H., Monaco, H. L. & Amzel, L. M. (1996). *Nature Struct. Biol.* **3**, 934–939.
Boissy, G., de La Fortelle, E., Kahn, R., Huet, J. C., Bricogne, G., Pernollet, J. C. & Brunie, S. (1996). *Structure*, **4**, 1429–1439.
Boissy, G., O'Donohue, M., Gaudemer, O., Perez, V., Pernollet, J. C. & Brunie, S. (1999). *Protein Sci.* **8**, 1191–1199.
Bonnet, P., Bourdon, E., Ponchet, M., Blein, J. P. & Ricci, P. (1996). *Eur. Plant Pathol.* **102**, 181–192.
Choinowski, T., Hauser, H. & Piontek, K. (2000). *Biochemistry*, **39**, 1897–1902.
Collaborative Computational Project, Number 4 (1994). *Acta Cryst.* D**50**, 760–763.
Demaret, S., Demaret, J. P. & Brunie, S. (2000). *J. Biomol. Struct. Dyn.* **18**, 453–460.
Fefeu, S., Birlirakis, N. & Guittet, E. (1998). *Eur. Biophys. J.* **27**, 167–171.
Fefeu, S., Bouaziz, S., Huet, J. C., Pernollet, J. C. & Guittet, E. (1997). *Protein Sci.* **6**, 2279–2284.
Fourme, R., Dhez, P., Benoit, J. P., Kahn, R., Dubuisson, J. M., Buisson, P. & Frouin, J. (1992). *Rev. Sci. Instrum.* **63**, 982–987.
Gooley, P. R., Keniry, M. A., Dimitrov, R. A., Marsh, D. E., Keizer, D. W., Gayler, K. R. & Grant, B. R. (1998). *J. Biomol. NMR*, **12**, 523–534.
Haapalainen, A. M., van Aalten, D. M., Merilainen, G., Jalonen, J. E., Pirila, P., Wierenga, R. K., Hiltunen, J. K. & Glumoff, T. (2001). *J. Mol. Biol.* **313**, 1127–1138.
Huet, J. C., Mansion, M. & Pernollet, J. C. (1993). *Phytochemistry*, **34**, 1261–1264.
Huet, J. C., Nespoulous, C. & Pernollet, J. C. (1992). *Phytochemistry*, **31**, 1471–1476.
Huet, J. C. & Pernollet, J. C. (1989). *FEBS Lett.* **257**, 302–306.
Huet, J. C. & Pernollet, J. C. (1993). *Phytochemistry*, **33**, 797–805.
Kamoun, S., Klucher, K. M., Coffey, M. D. & Tyler, B. M. (1993). *Mol. Plant Microbe Interact.* **6**, 573–581.
Keller, H., Pamboukdjian, N., Ponchet, M., Poupet, A., Delon, R., Verrier, J. L., Roby D. & Ricci, P. (1999). *Plant Cell*, **11**, 223–235.
Kraulis, P. E. (1991) *J. Appl. Cryst.* **24**, 946–950.
Lamzin, V. S. & Wilson, K. S. (1997). *Methods Enzymol.* **277**, 269–305.
Landon, C., Berthault, P., Vovelle, F. & Desvaux, H. (2001). *Protein Sci.* **10**, 762–770.
Lascombe, M. B., Milat, M. L., Blein, J. P., Panabières, F., Ponchet, M. & Prangé, T. (2000). *Acta Cryst.* D**56**, 1498–1500.
Laskowski, R. A., McArthur, M. W., Moss, D. S. & Thornton, J. M. (1993). *J. Appl. Cryst.* **26**, 283–291.
Leslie, A. G. W. (2001). *MOSFLM: Program for Autoindexing and Integrating X-ray Diffraction Data*, Version 6.11. MRC Laboratory of Molecular Biology, Hills Road, Cambridge.
Merritt, E. A. & Bacon, D. J. (1997). *Methods Enzymol.* **277**, 505–524.
Mikes, V., Milat, M. L., Ponchet, M., Panabières, F., Ricci, P. & Blein, J. P. (1998). *Biochem. Biophys. Res. Commun.* **245**, 133–139.
Mikes, V., Milat, M. L., Ponchet, M., Ricci, P. & Blein, J. P. (1997). *FEBS Lett.* **4**, 190–192.
Mouton-Peronnet, F., Bruneteau, M., Denoroy, L., Boulieau, P., Ricci, P., Bonnet, P. & Michel, G. (1995). *Phytochemistry*, **38**, 41–44.
Navaza, G. (1994). *Acta Cryst.* A**50**, 157–163.
Nicholls, A., Sharp, K. & Honig, B. (1991). *Proteins Struct. Funct. Genet.* **11**, 281–296.
Osman, H., Mikes, V., Milat, M. L., Ponchet, M., Marion, D., Prangé, T., Maume, B. F., Vauthrin, S. & Blein, J. P. (2001). *FEBS Lett.* **489**, 55–58.
Osman, H., Vauthrin, S., Mikes, V., Milat, M. L., Panabières, F., Marais, A., Brunie, S., Maume, B., Ponchet, M. & Blein, J. P. (2001). *Mol. Biol. Cell.* **12**, 2825–2834.
Ponchet, M., Panabières, F., Milat, M. L., Mikes, V., Montillet, J. L., Suty, L., Triantaphylides, C., Tirilly, Y. & Blein, J. P. (1999). *Cell Mol. Life Sci.* **56**, 1020–1047.
Prangé, T., Pernot, L., Colloc'h, N., Longhi, S., Bourguet, W., Fourme, R. & Schiltz, M. (1998). *Proteins Struct. Funct. Genet.* **30**, 61–73.
Quillin, M. L., Breyer, W. A., Grisworld, I. J. & Matthews, B. W. (2000). *J. Mol. Biol.* **302**, 955–977.
Ramachandran, G. N., Ramakrishnan, C. & Sasisekharan, V. (1963). *J. Mol. Biol.* **7**, 95–99.
Ricci, P., Bonnet, P., Huet, J. C., Sallantin, M., Beauvais-Cante, F., Bruneteau, M., Billard, V., Michel, G. & Pernollet, J. C. (1989). *Eur. J. Biochem.* **183**, 555–563.
Sheldrick, G. M. & Schneider, T. R. (1997). *Methods Enzymol.* **277**, 319–343.
Vauthrin, S., Mikes, V., Milat, M. L., Ponchet, M., Maume, B., Osman, H. & Blein, J. P. (1999). *Biochem. Biophys. Acta*, **19**, 335–342.
Vincent, F., Spinelli, S., Ramoni, R., Grolli, S., Pelosi, P., Cambillau, C. & Tegoni, M. (2000). *J. Mol. Biol.* **300**, 127–139.